Jetpack Arrest Mechanism (JAM)
MAE 154A Final Project Report

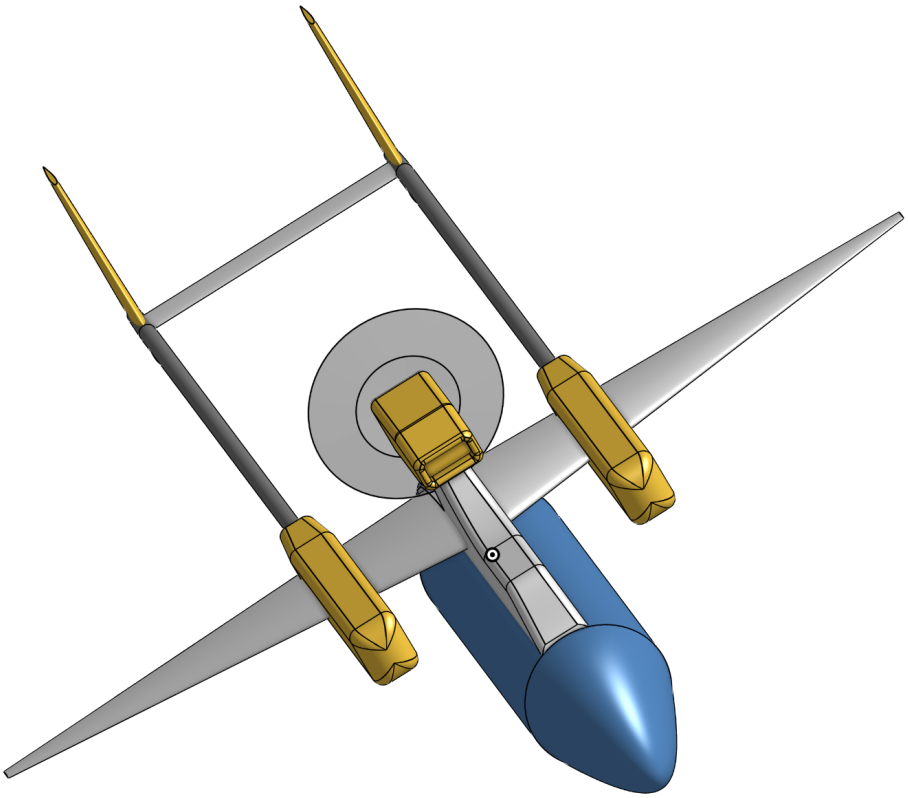

James Tseng, Daniel Lin, and Allan Zhao
Group Two

UCLA Henry Samueli School of Engineering
Los Angeles, California

Table of Contents

1. Introduction

In mid 2020, airline pilots flying into Los Angeles International Airport (LAX) reported observing a jetpack flying in airspace near the runway. Aerial intruders, such as this jetpack sighting, pose a significant risk to any airplane taking off or landing as airplane engines are uniquely vulnerable to collisions with these flying objects. As a result of the reported jetpack sightings, LAX was forced to close its runways for a short period of time. Closing a major airport such as LAX can cost the economy millions of dollars and should be avoided at all costs.

Image 1. Photograph of the purported jetpack near the Palos Verdes Peninsula.

2. Mission Requirements

An unmanned aerial vehicle (UAV) can potentially prevent and catch aerial intruders flying into LAX's restricted airspace. This UAV would need to take off from its base of operations, fly to the designated "hunt area", catch the aerial intruder, and fly and land back at its origin. An UAV is ideal for this mission since it eliminates the need for a pilot to be on standby—any time an aerial intruder flies into restricted airspace, the UAV can be deployed to catch this trespasser.

a. Flight Requirements

In order for the UAV to be able to catch this aerial intruder, it must be maneuverable and fast to capture its nimble target. The UAV must also have a sufficiently large range and long flight time for the UAV to have a

reasonable operational area. Table 1 below details some of the flight requirements of the UAV.

Range	200 miles round-trip
Hunting time	1 hour
Maximum speed	80 miles per hour
Climb rate	500 feet per minute

Table 1. List of minimum flight requirements for the UAV.

b. Payload

The payload that the UAV must carry can be split into two parts: the equipment needed to fly to and track the jetpack and the weight of the jetpack when the UAV flies back to its base of operations.

The UAV must also be able to carry certain equipment to catch the aerial intruder. Since the UAV will be flying from LAX, it must carry communication and transponder equipment for it to safely navigate the crowded airspace in Los Angeles. The UAV will also need to carry the required avionics for autonomous flight to be possible. In total, this was estimated to weigh around 30 pounds.

In addition to the equipment required for the UAV to fly its mission, it must also be capable of carrying the jetpack back to base inside its fuselage after it has caught the aerial intruder. This payload will only be carried for the return flight and is estimated to weigh 500 pounds.

3. Engine Selection

The engine used for the UAV must be light but also able to output a significant power for the airplane to be able to carry the jetpack man back to the UAV base. Jet engines were not considered for this UAV design since the UAV will not achieve a high enough speed for jet engines to become economical, and propeller propulsion systems are less complex and more commonly used for airplanes of this size compared to jet engines.

a. Candidates

The primary consideration for the UAV engine was the horsepower since the engine must be able to provide enough power to complete the mission. After a few iterations, it is determined that the weight of the engine is essential to optimizing the final weight of the aircraft since it is a significant fraction of the total weight. The engine candidates are selected based on research on similarly sized general aviation aircraft, such as the Cessna 150 and Cessna 172. Ultimately, seven engine candidates were used in the Monte Carlo optimization script (detailed in section nine of this report) for determining the engine used in the final UAV design. The specifications of these engines are shown in table two below.

Engine	Weight (lbs)	Horsepower	C_p (lb/(hp*hr))	Dimensions (ft) Length x Diameter
UL Power UL520iS	238	200	0.4435	2.3667 x 1.9821
Viking 150	239	150	0.3957	2.25 x 1.9167
TurbAero TA200TP Talon	270	190	0.57	3.0583 x 1.3833
Continental IO-360	330	190	0.4632	3.333 x 2.5417
Lycoming IO-360-B	330	200	0.4	2.5 x 2.25
Austro Engine AE300	410	168	0.3667	2.42 x 1.9821
Austro Engine AE330	410	180	0.3813	2.42 x 1.9821

Table 2. Specifications of engines considered for UAV design.

b. Viking 150

The Monte Carlo optimization script determined that the best engine for JAM is the Viking 150 engine. This engine is a four-cylinder, four-stroke, aluminum, gasoline engine that can produce 150 horsepower at 5,800 revolutions per minute.

The Viking 150 engine is one of the lightest engines in the candidate pool. This results in a high horsepower to weight ratio, but it does not have the highest ratio out of all the candidate engines (the highest being the UL520iS engine). The Viking 150 engine is likely preferred compared to the UL520iS engine because of its higher efficiency as seen in its thrust specific fuel consumption, C_p value. Even though the Viking 150 cannot output as much power as the UL520iS, it requires less fuel to generate a comparable amount of horsepower. With the Viking 150, the UAV would need to carry less fuel to meet its range and endurance requirements, resulting in a lower weight.

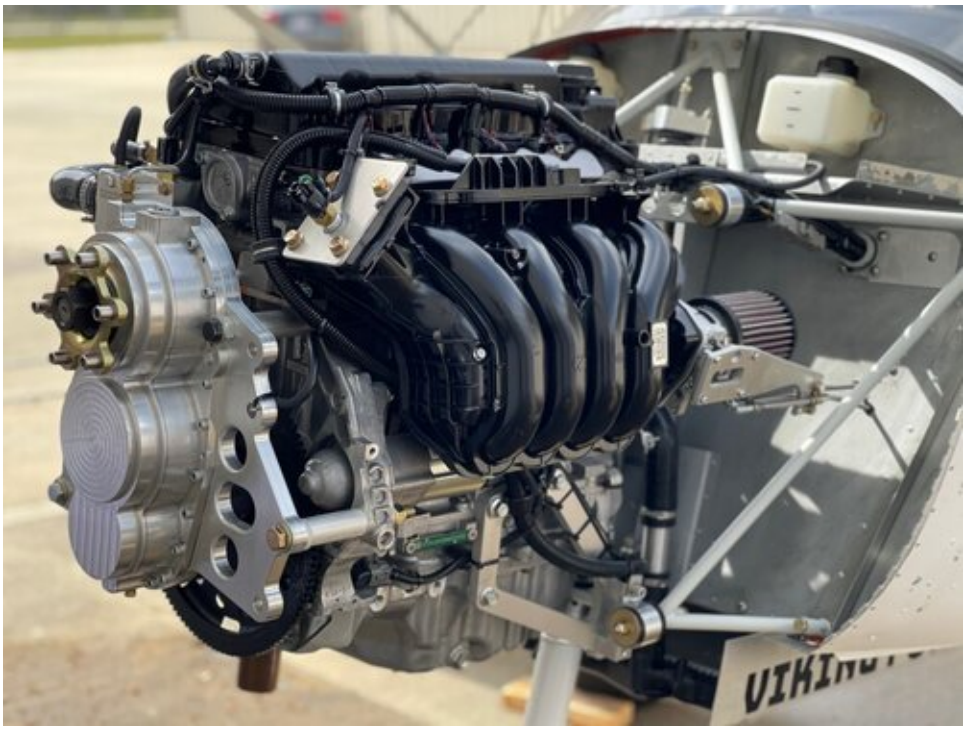

Image 2. A manufacturer-provided image of the Viking 150 engine.

4. Propeller Selection

Since the UAV is not utilizing jet propulsion, it is necessary to find an appropriate propeller blade design to use in combination with the engine selected in section three above. The final propeller choice was determined using the Monte Carlo optimization script.

a. Candidates

Ultimately, four possible propeller designs were considered from the NACA 640 report: the two and three bladed Clark Y and the two and three bladed RAF Six.

b. Three Blade Clark Y

After running the Monte Carlo optimizations, the three bladed Clark Y propellers is used in the final UAV design. While 3-bladed propellers are less efficient than 2-bladed propellers, they're able to output more thrust when provided the same power. To determine the efficiency of the propeller, the C value of the propeller can be found via:

$$C_s = \sqrt[5]{\frac{\rho V^5}{P n^2}} \quad (1)$$

Where ρ is the density of air, V is the aircraft speed, P is engine power output, and n is the rotational speed of the shaft. For the UAV's design cruise speed of 80 miles per hour, the C value is calculated to be 0.585. The advanced ratio can then be found using the following equation:

$$J = \frac{V}{nD} \quad (2)$$

With D being the diameter of the propeller, the advanced ratio, J, is determined to be 0.773. J and C can then be used to find the propeller blade angle using figure one on the next page. The UAV is designed with a variable pitch propeller blade. For simplicity, the blade angles are restricted from 15 degrees to 45 degrees to correspond to the curves presented in the NACA 640 report. At cruise conditions, the blade angle resolves to roughly 25 degrees.

Finally, the propeller efficiency can be found on figure two of the NACA 640 report. The UAV, with its propeller blade angle of 25 degrees and advanced ratio of 0.773 has a propeller efficiency around 0.823.

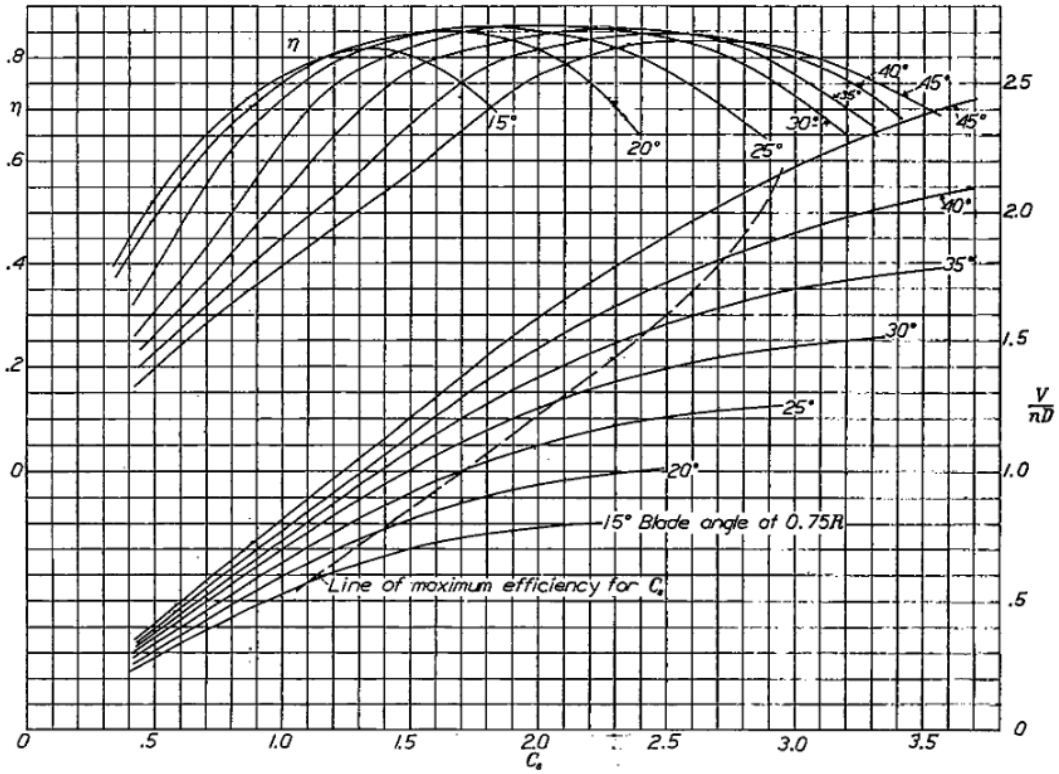

Figure 1. Design chart for three blade Clark Y propellers.

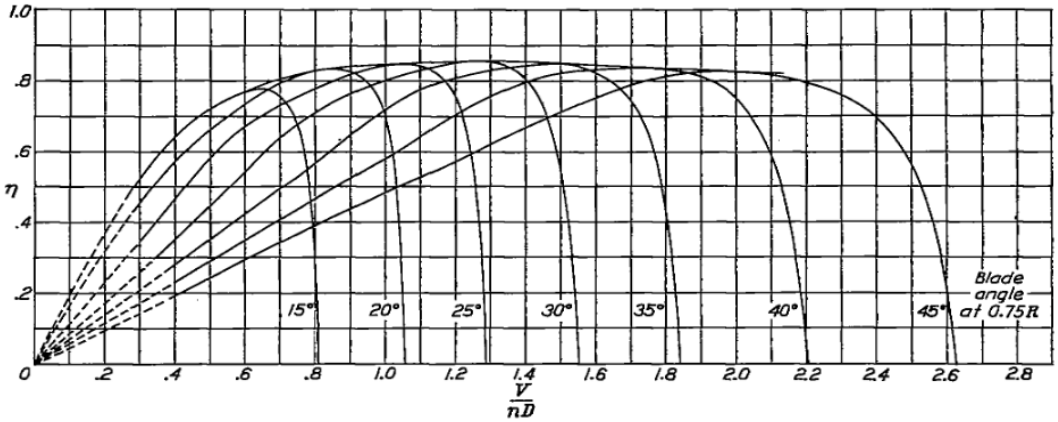

Figure 2. Efficiency curves for three blade Clark Y propellers.

5. Airfoil Selection

JAM must have an appropriate wing and airfoil to generate the lift for the aircraft to meet performance requirements. The airfoil design process is similar to the engine selection process discussed in section three above: candidate airfoils were selected and inputted into the Monte Carlo optimization script. A final airfoil was then selected for use in the optimal UAV design.

a. Candidates

The airfoils used in the Monte Carlo optimization script were chosen based off of aircraft that have similar size, weight, and performance to the mission parameters for this UAV design. Six different airfoils were tested in the Monte Carlo optimization: the NACA 0012, 1408, 2412, 4412, 6409, and 22112 airfoils.

b. NACA 0012

Most of the iterations in the Monte Carlo script determined that the NACA 0012 airfoil was the ideal choice for the UAV. The NACA 0012 airfoil has max lift to drag ratio of 25.67 at an angle of attack of five degrees. Figures 3 and 4 below and on the next page show characteristics of this airfoil as determined by xfoil software. The NACA 0012 airfoil was likely selected over other airfoils due to its symmetric form generating less induced drag. This allows the aircraft to perform more efficiently in the lower speeds where the induced drag dominates.

It is worth noting that the NACA 2412 airfoil also passed performance requirements and would occasionally be selected by the Monte Carlo optimizations. It produces more lift than the NACA 0012 at the cost of additional drag. This means although it can reach performance requirements similarly to the NACA 0012, it'll need more power, meaning more fuel for the aircraft to operate. The NACA 0012 was ultimately the more common output of the Monte Carlo optimization because it still satisfies JAM's performance requirements but with a lower power requirement.

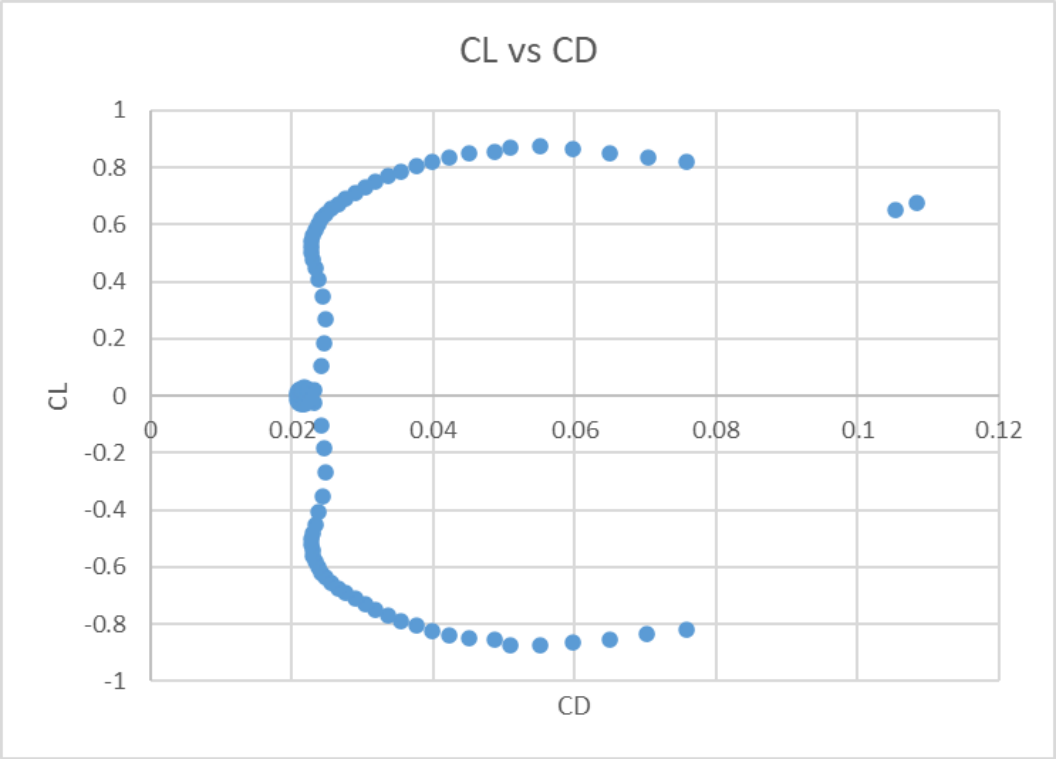

Figure 3. Drag and lift coefficients of the NACA 0012 airfoil.

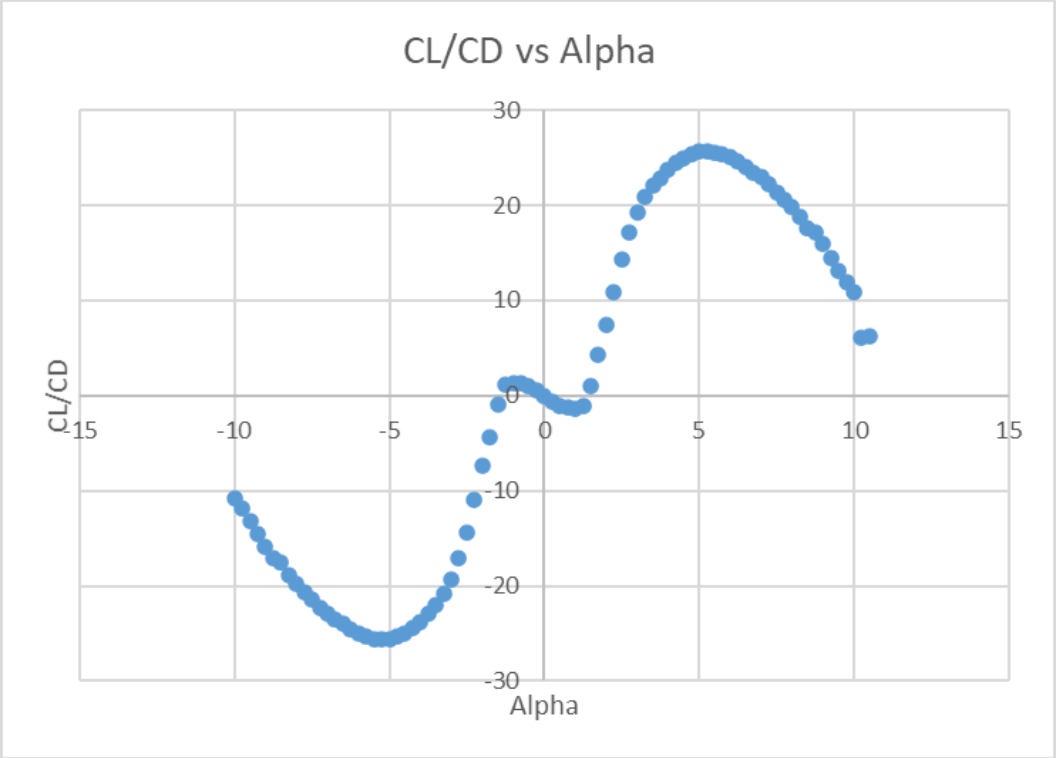

Figure 4. Lift drag curve for the NACA 0012 airfoil.

6. Nicolai Weight Estimation

The next component of designing the UAV was estimating an initial weight for the aircraft. This weight estimation is vital for calculating the lift, drag, and power required for the UAV. This was done through iteration and use of the Nicolai equations.

The first step of this process was to determine an initial guess weight. Through research of planes with similar flight performances to the mission requirements, the guess weight was set at 2,700 pounds. The weight is then used with the lift equation (equation three below) to calculate the lift coefficient of the UAV.

$$W = L = \frac{1}{2}\rho V^2 s \tag{3}$$

Where s is the reference area of the UAV wing.
The iterative process continues with estimations of the drag through the component build up method. This method calculates the overall drag of an aircraft system by summing up each components' contribution to the parasitic drag using the following equation:

$$C_{D_P} = \sum_{i=1}^{\#components} \frac{K_i Q_i C_{f_i} S_{wet_i}}{S_{ref}} \tag{4}$$

Where C_{D_p} is the parasitic drag coefficient of the UAV, K_i is form factor of the component, Q_i is the interference factor of the component, c_{f_i} is the skin friction coefficient of the component, S_{wet_i} is the wetted area of the component, and S_{ref} is the reference (wing) area of the UAV.

The skin friction coefficient for each component can be calculated using the following equation:

$$C_f = \frac{0.455}{(log_{10}Re)^{2.58}(1+0.144M^2)^{0.65}} \tag{5}$$

Where Re is the local Reynolds number and M is the Mach number of the flow.

The form factor can be determined using one of the following equations:

$$K = \left[1 + \frac{0.6}{(x/c)_m}\left(\frac{t}{c}\right) + 100\left(\frac{t}{c}\right)^4\right]\left[1.34M^{0.18}cos\left(\Lambda_m\right)^{0.28}\right] \tag{6}$$

$$K = \left(1 + \frac{60}{f^3} + \frac{f}{400}\right) \quad (7)$$

$$f = \frac{l}{Diam} \quad (8)$$

Equation six is used to find the form factor of any lifting surface and equations seven and eight are used for any object that can be approximated as a smooth cylinder. $(x/c)_m$ is the location along the airfoil where the airfoil is thickest, t is the thickness of the airfoil, c is the chord length of the airfoil, Λ_m is the wing sweep angle, l is the length of the smooth cylinder, and D is the diameter of the smooth cylinder.

After calculating the parasitic drag of the UAV, the induced drag produced by the UAV's lift needs to be calculated. This can be found using:

$$C_{D,i} = \frac{C_{L_w}^{\ 2}}{\pi A_w e_w} + \frac{S_t}{S_w}\frac{C_{L_t}^{\ 2}}{\pi A_t e_t} \quad (9)$$

C_L is the lift coefficient for the lifting surface, S is the surface area of the lifting surface. A is the aspect ratio of the lifting surface, and e is the Oswald efficiency, approximated based on the wing sweep and aspect ratio. The t and w subscripts designate the tail and wing components respectively.

After the parasitic and induced drag coefficients are calculated, they can be simply combined to find the total drag coefficient of the UAV. The drag and power required can then be calculated via:

$$D = \frac{1}{2}\rho V^2 S C_D = \frac{1}{2}\rho V^2 S\left(C_{D_p} + C_{D_i}\right) \quad (10)$$

$$P_{req} = DV \quad (11)$$

With this calculated, the weights of the UAV components can be calculated. First, the aircraft mission requirements are used to find the required fuel that the UAV must carry. This is done through the Breguet range and endurance equations:

$$R = \frac{n_{pr}}{c_p}\frac{C_L}{C_D} ln\left(\frac{w_i}{w_f}\right) \quad (12)$$

$$E = \frac{n_{pr} C_L^{\ 3/2}}{c_p C_D}\sqrt{2\rho S}\left(\frac{1}{w_f^{\ 1/2}} - \frac{1}{w_i^{\ 1/2}}\right) \quad (13)$$

Where n_{pr} is propeller efficiency, c_p is the specific fuel consumption, and w_i and w_f are the initial and final weights respectively.

The weights of the aircraft components can be found using the following:

$$W_{wing} = 96.948\left[\left(\frac{W_{TO}N}{10^5}\right)^{0.65}\left(\frac{A}{\cos\Lambda_m}\right)^{0.57}\left(\frac{S_w}{100}\right)^{0.61}\left(\frac{1+\lambda}{2t/c}\right)^{0.36}\left(1+\frac{V_e}{500}\right)^{0.5}\right]^{0.993} \quad (14)$$

$$W_{fues} = 200\left[\left(\frac{W_{TO}N}{10^5}\right)^{0.286}\left(\frac{l}{10}\right)^{0.857}\left(\frac{w+Diam}{10}\right)\left(\frac{V_e}{100}\right)^{0.338}\right]^{1.1} \quad (15)$$

$$W_{horz\ tail} = 127\left[\left(\frac{W_{TO}N}{10^5}\right)^{0.87}\left(\frac{S_H}{100}\right)^{1.2}\left(\frac{l_t}{10}\right)^{0.483}\left(\frac{b_H}{t_{HR}}\right)^{0.5}\right]^{0.458} \quad (16)$$

$$W_{vert\ tail} = 98.5\left[\left(\frac{W_{TO}N}{10^5}\right)^{0.87}\left(\frac{S_V}{100}\right)^{1.2}\left(\frac{b_V}{t_{VR}}\right)^{0.5}\right]^{0.458} \quad (17)$$

$$W_{LG} = 0.054\left(L_{LG}\right)^{0.501}\left(W_{land}N_{land}\right)^{0.694} \quad (18)$$

$$W_{prop\ unit} = 2.575\left(W_{engine}\right)^{0.922}N_E \quad (19)$$

$$W_{fuel\ system} = 2.49\left[\left(F_G\right)^{0.6}\left(\frac{1}{1+Int}\right)^{0.3}\left(N_T\right)^{0.2}\left(N_E\right)^{0.13}\right]^{1.21} \quad (20)$$

$$W_{surface\ controls} = 1.066\left(W_{TO}\right)^{0.626} \quad (21)$$

N is the ultimate load factor (assumed to be 6.6), λ is the taper ratio, V_e is the max speed in knots, l_t is the distance between the tail and wing quarter chords, b is the span of the airfoil, L_{LG} is the length of the landing gear in inches, N_E is the number of engines, Int is the percentage of fuel tanks that are integral (assumed to be 100 percent in this project), and N_T is the number of fuel tanks. These weights can then be summed with the payload weight, the fuel weight, and avionics and other equipment weight to find this iterative step's weight estimate.

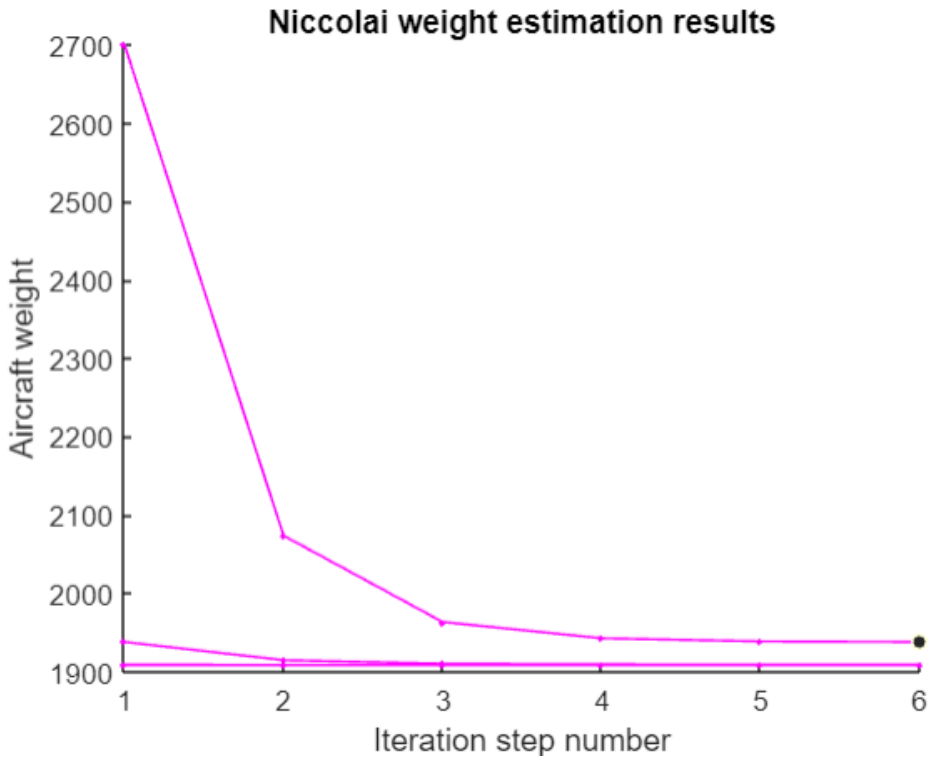

Figure 5. Evolution of aircraft weight estimates produced by Nicolai equations.

The initial estimation of aircraft weight was 2700 pounds, based on the preliminary requirements driven design. Applying the Nicolai method with the Monte Carlo optimizations converges the weight to 1,938 pounds, 800 pounds lighter than the initial estimate.

7. Aircraft Geometry

The aircraft was designed and modeled using Onshape computer design software. The following tables and figures provide important aircraft design specifications and characteristics.

S_{wing}	52.8592 sq. ft
b_{wing}	14.8713 ft
Wing airfoil	NACA 0012
Wing chord	6.95 ft
Wing taper ratio	0.0231
Wing sweep	0.1720 deg
Wing aspect ratio	8.3678
$S_{horizontal\ stabilizer}$	16.3041 sq. ft
$b_{horizontal\ stabilizer}$	9.4356 ft
Horz. stab. airfoil	NACA 0012
Horz. stab. chord	1.73 ft
Horz. stab. sweep	0 deg
Horz. stab. aspect ratio	5.4607

$S_{vertical\ stabilizer}$	8.5212 sq. ft
$b_{vertical\ stabilizer}$	7.0241 ft
Vert. stab. airfoil	NACA 0012
Vert stab. chord	2.43 ft
Vert. stab. sweep	19.0560 deg
Vert. stab. aspect ratio	5.4607

Fuselage length	22 ft
Fuselage diameter	2.25 ft

Tail boom length	22.0876 ft

Aircraft weight	1,546 lb
Length	40 ft
Width	31.34 ft
Height	11.9420 ft

Table 4. The physical geometry of the UAV.

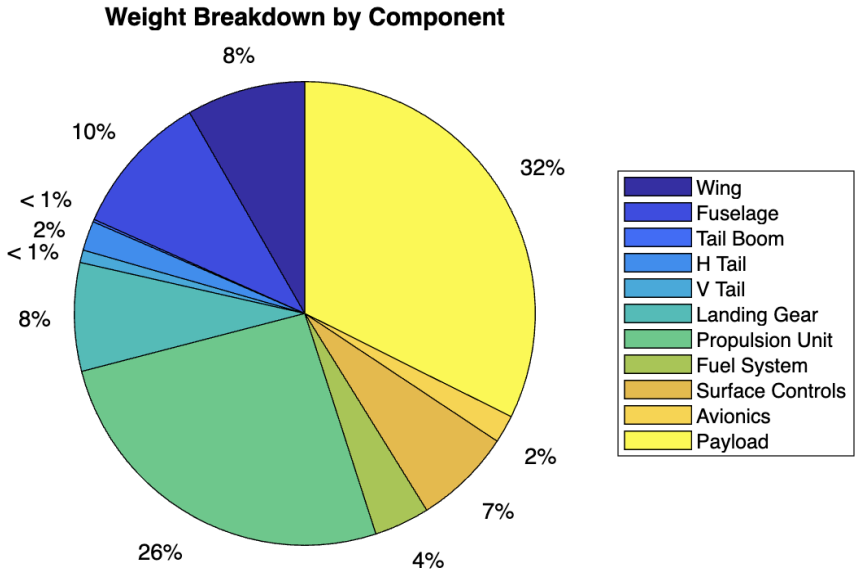

Figure 6. Pie chart of each components' contribution to the overall weight.

Component	Weight (lb)	CG distance (ft)
Wing	128.8332	5.5
Fuselage	154.8890	2
Tail boom	2.6829	7.725
Horizontal stabilizer	31.8930	15.45
Vertical stabilizer	13.4977	15.45
Landing gear	116.8511	4.45
Power unit	401.4765	2.5
Fuel system	60.0082	5.5
Surface controls	105.7256	5.5
Avionics	30.0	1.5
Payload	500.0	1

Table 5. Weights and center of gravity locations of aircraft components. CG distance is measured from the wing root leading edge.

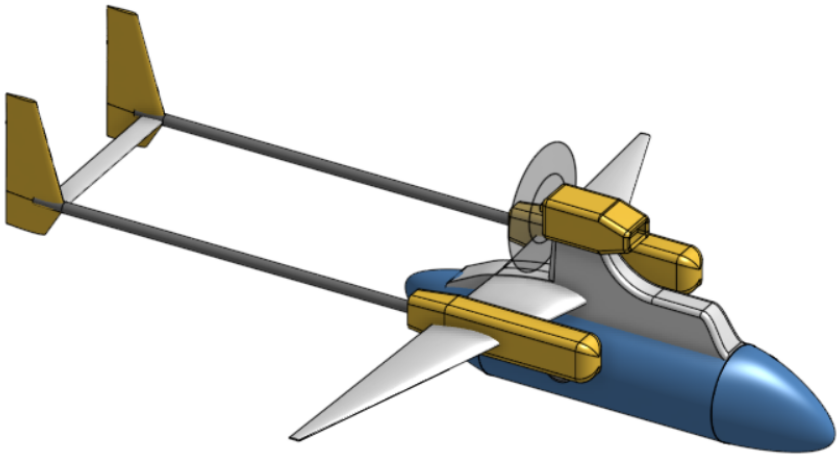

Image 3. Isometric view of the final UAV design.

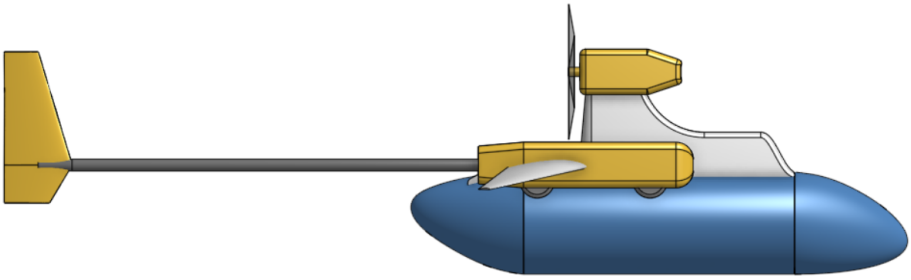

Image 4. Side view of the final UAV design.

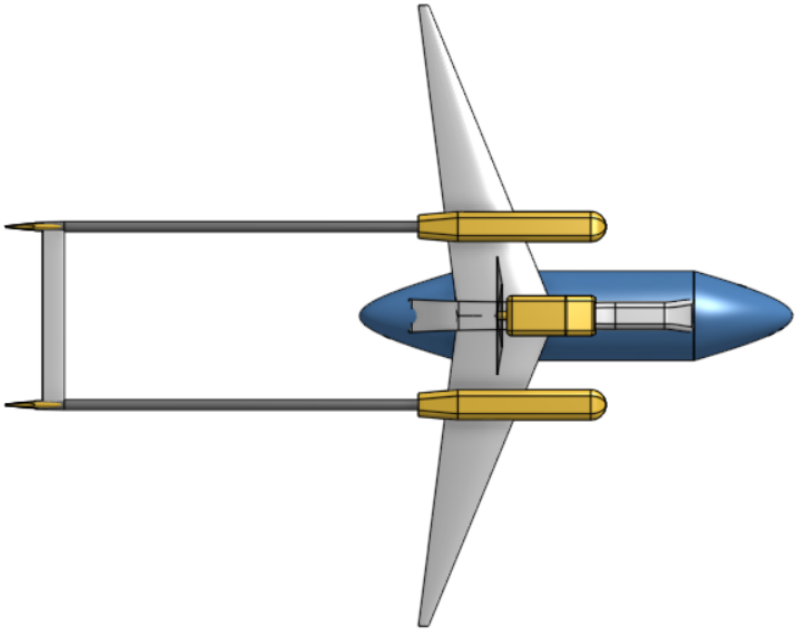

Image 5. Top view of the final UAV design.

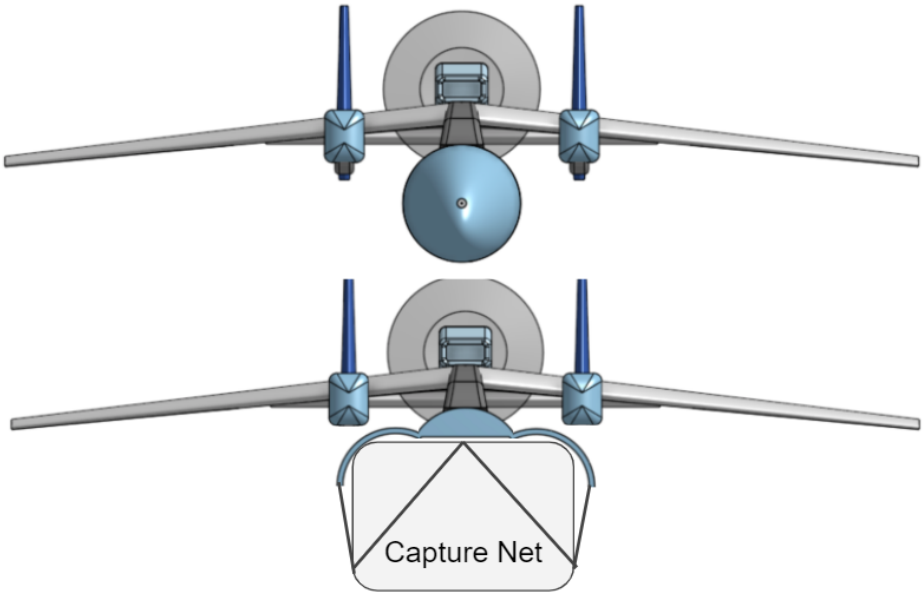

Image 6. Front view of the UAV with capture mechanism hidden and shown.

The engine and propeller are mounted over the fuselage to provide more clearance for the jetpack capture net down below. The jetpack capture net is stored within the fuselage while tracking the jetpack person's location. Once the aircraft has approached the jetpack person, the capture net will be deployed and the aircraft will perform maneuvers to apprehend the jetpack person. The capture net will then retract the jetpack person back into the fuselage for the return trip to LAX.

Initially, the Monte Carlo optimization would vary multiple geometries randomly, allowing us to produce an aircraft with a much lower total weight than the final design. However, this would produce absurd geometries such as extremely long tail booms or very small wings. To remedy this, geometry constraints were placed on the randomized parameters so that the Monte Carlo iterations wouldn't produce unreasonable values.

As discussed earlier, the payload and fuel systems comprise the majority of the weight, meaning that optimizing either the payload or fuel system would significantly reduce the aircraft's total weight.

8. Stability

The aircraft must be statically stable for both regimes of flight: without the payload flying to the jetpack suspect, and with the suspect stowed as payload in the aircraft. The UAV was modeled in both conditions and must be statically stable in order to pass the stability requirement. For the optimal aircraft, the stability criteria are tabulated below in Table 6.

	No Payload	Payload
Center of Gravity	0.5820	0.4403
Neutral Point	0.8603	0.8603
Static Margin	0.2783	0.4200
C_{M_alpha}	-0.0239	-0.0361

Table 6. Stability criteria of optimal UAV. Distances of center of gravity, static margin, and static margin are measured from the wing root leading edge and are dimensions with respect to wing chord length.

It is interesting to note that the static stability criteria improved with the addition of the payload, which is due to the center of gravity of the payload being forward of the center of gravity of the aircraft as a whole. This is confirmed by the center of gravity decreasing with the addition of the payload.

With regards to dynamic stability derivatives, portions of the stability derivatives were calculated. The remaining derivatives were to be determined with numerical methods, such as using VSPAERO or DATCOM on the optimal aircraft geometry, which the team did not have sufficient resources to achieve. The derivatives that were calculated are tabulated below.

	No Payload	Payload
CL0	0	0
CL_a	4.9199	4.9199
CL_adot	2.6747	2.7707

CL_q	5.1925	5.3790
CL_de	0.6578	0.6578
CD0	0.0650	0.0650
CD_a	0.6156	0.6156
CD_de	0.0261	0.0261
Cm0	0.3103	0.4852
Cm_a	-1.3693	-2.0664
Cm_adot	10.5561	11.3277
Cm_q	-20.4935	-21.9915
Cm_de	-2.5963	-2.6895

Table 7. Calculated stability derivatives of optimal aircraft.

The stability derivatives of the optimal aircraft are at most an order of magnitude in difference from the Pioneer UAV's stability derivatives, as a benchmark of comparison.

9. Flight Performance

The aircraft geometry and lift produced by the wing was used to calculate the drag of the UAV using equations four through ten in section six above. The following figure shows the drag of the aircraft as a function of velocity. The drag changes when the UAV captures the aerial object. This is because the induced drag increases as the wing needs to create more lift to counter the increased weight of the aircraft. The parasitic drag remains the same as the aircraft geometry remains unchanged.

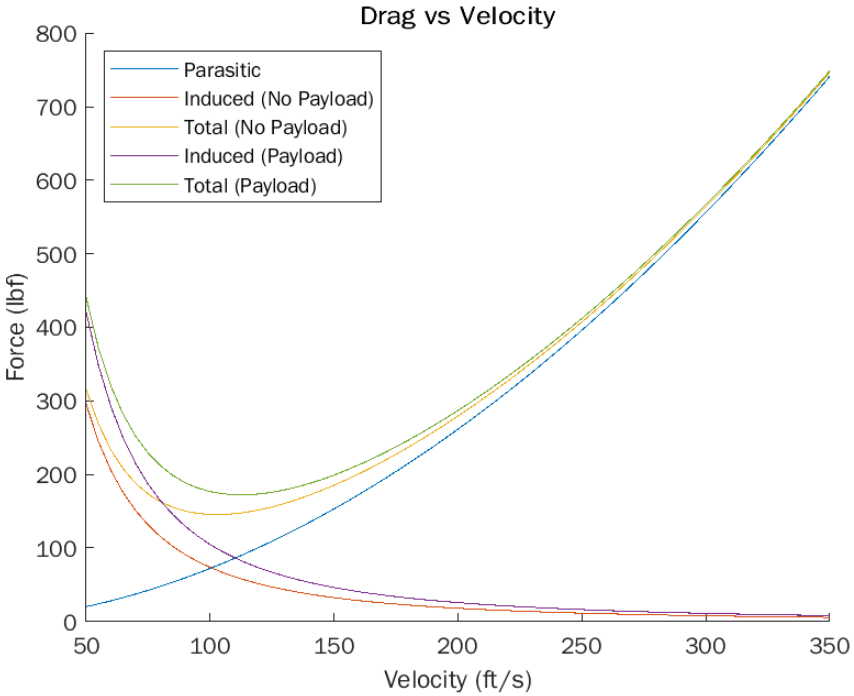

Figure 7. Contributions to UAV drag by parasitic and induced sources.

With the drag calculated, the power required to fly the UAV can be simply calculated using equation 11. The power outputted by the engine selected can also be plotted along with the required power to produce the following graph:

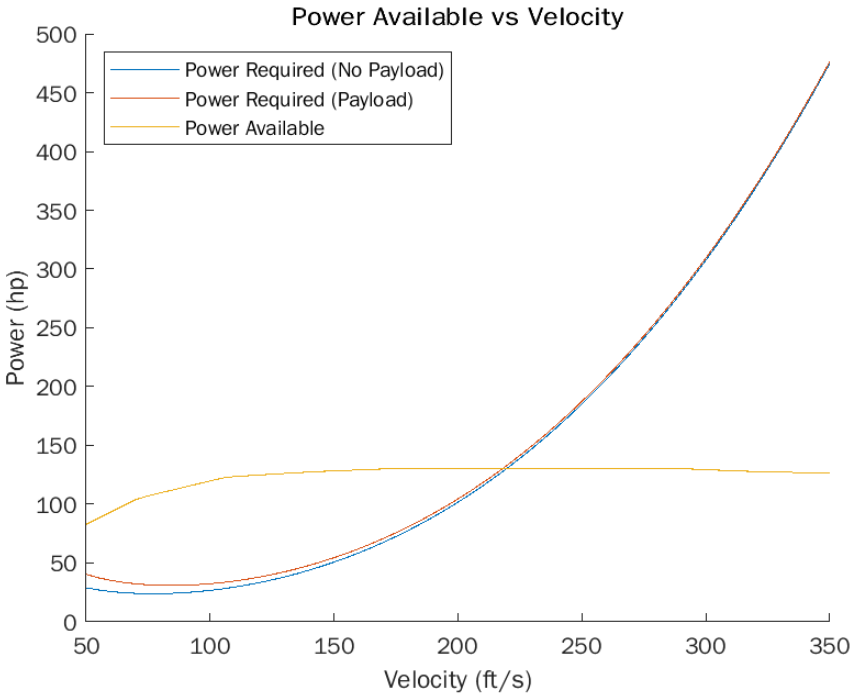

Figure 8. Power curves for the UAV.

These two graphs provide important information regarding the airplane flight characteristics. Since the power required exceeds the power output by the engine at a velocity of 220 feet per second, the aircraft's maximum velocity would be 150 miles per hour. This maximum velocity exceeds the required maximum velocity established in the mission parameters. The cruise speed of the aircraft can also be calculated by finding the velocity where drag is at a minimum; using figure seven, the aircraft cruise velocity is around 110 feet per second, or 75 miles per hour.

The power curve can also be used to calculate the maximum climb rate. Aircraft climb fastest at the velocity where the excess power is maximized. From figure eight, this occurs around 120 feet per second. The climb rate can then be calculated using the following equation:

$$RC = \frac{P_{av} - P_{req}}{W} \tag{22}$$

Where RC is the rate of climb, P_{av} is the power available from the engine, P_{req} is the power required to fly the plane from equation 11, and W is the weight of the aircraft. Plugging in the appropriate values when the aircraft is flying at 120 feet

per second yields a maximum climb rate of 3,192 feet per second. This climb rate is significantly larger than the mission requirements. The large climb rate indicates that the UAV will be highly maneuverable, and it will be able to capture the flying jetpack with minor difficulty.

The drag chart that was calculated in figure seven can also be used to determine lift over drag curves. These are shown in figure nine.

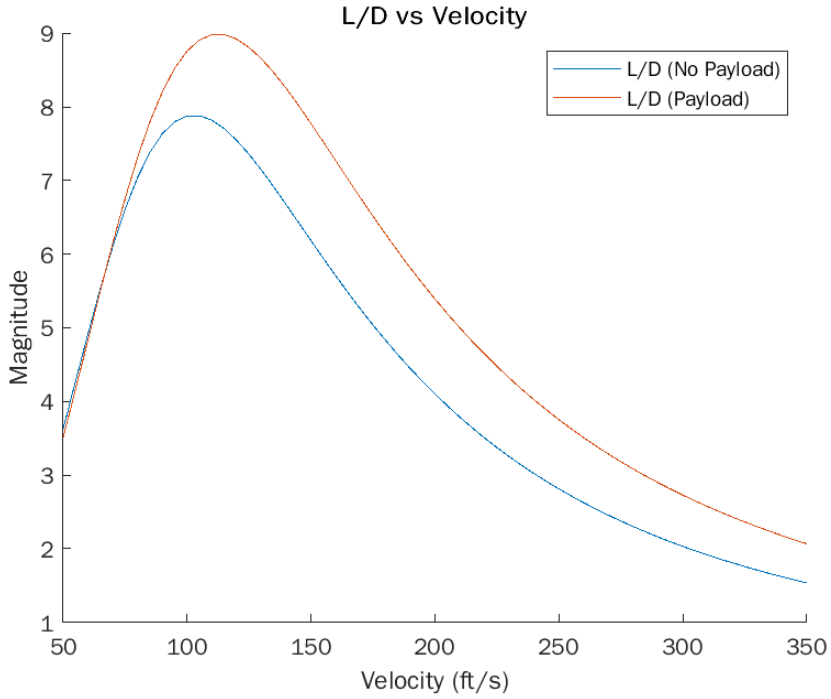

Figure 9. Lift over drag curves for the UAV.

10. Optimization and Monte Carlo Method

The UAV is optimized using an iterative Monte Carlo approach scripted in MATLAB. The randomization and optimization procedure takes inspiration from model training procedures in machine learning. The optimization process as a whole is summarized in Table 8 below.

Number of iterations	20,000
Number of epochs	5
Random distribution	Linear, Gaussian

Aircraft parameters randomized			
Tail boom length	Wing chord	Wing span	Wing taper ratio
Wing sweep angle	V tail chord	V tail span	V tail sweep angle
H tail chord	H tail span	Engine choice	Fuel capacity
Wing airfoil choice		Prop choice	Prop diameter

Table 8. Summary of iteration process and aircraft parameters randomized.

For each iteration, the aircraft's parameters are randomized around the current best aircraft (lowest in weight). The first iteration is based on the aircraft parameters derived from the requirements constrained approach.

The epochs are a method of regularization that prevents the Monte Carlo iteration from converging onto a local minima of best lowest weight aircraft. The current best aircraft is reset to the default (from the requirements constrained approach), which essentially restarts the Monte Carlo optimization. This practically yields 5 separate Monte Carlo optimizations.

The aircraft parameters are randomized through a linear and Gaussian random number generator such that the first half of the iteration in an epoch uses the linear random distribution, while the second half uses the Gaussian random distribution. The design choice is to randomize to a finer resolution in the second half of the epoch where a lower weight aircraft is likely found, and small adjustments to it via a Gaussian distribution is likely to assist finding an even lighter aircraft.

a. Optimization and Iterative Process

This section will detail the methodology of a single iteration in the Monte Carlo method of optimization.

First a new aircraft is generated with the aircraft parameters randomized around the previous best aircraft as described above, with the parameters listed in Table 6. During this step, a random engine and propeller was chosen from the options listed in sections three and four respectively.

The next step was to calculate the weights of each component in the aircraft. This was done using the Nicolai equations discussed in section six.

The script then calculates the aerodynamic coefficients of the aircraft. This includes the lift curve slopes for the wing and the horizontal stabilizer. The lift coefficient is also found in this module along with the angle of attack for the aircraft for cruise flight.

Stability coefficients and centers of gravity are then calculated for the aircraft. In this section, the most important calculation is for the neutral point and static margin of the aircraft. If the aircraft is determined to be unstable from these two values, then the iteration is designated as unstable and no further calculations are performed for this aircraft. A new iteration is started with a new randomly generated aircraft. Otherwise, the iteration is considered stable and it continues through the loop.

After the stability is calculated, the script calculates the lift and drag values of the aircraft. This is done using the component build up method that was also used in the Nicolai weight estimation.

Finally, the performance calculations are done for the aircraft. This step will calculate the fuel needed to fulfill the mission requirements as well as calculate the climb rate of the aircraft to see if it can fulfill flight requirements. If the iteration's aircraft can fulfill these requirements and has the lowest weight of any iteration, it will be designated the best aircraft.

b. Results

At the end of the entire optimization process, the optimized aircraft weight was decreased to 1,546 pounds from the initial requirements constrained approach aircraft of 2,000 pounds. More information about the final aircraft generated by the optimization process can be found in section eight above.

Every iteration is recorded to determine if it fulfills mission requirements and is stable for flight. The breakdown is tabulated below. This can be seen in the figures below that show the results of each iteration.

Percentage Pass	11.95%
Percentage Fail - Stability	56.01%
Percentage Fail - Requirements	68.03%

Table 9. Breakdown of iterations. The percentage of aircraft that are unstable and fail requirements are not mutually exclusive.

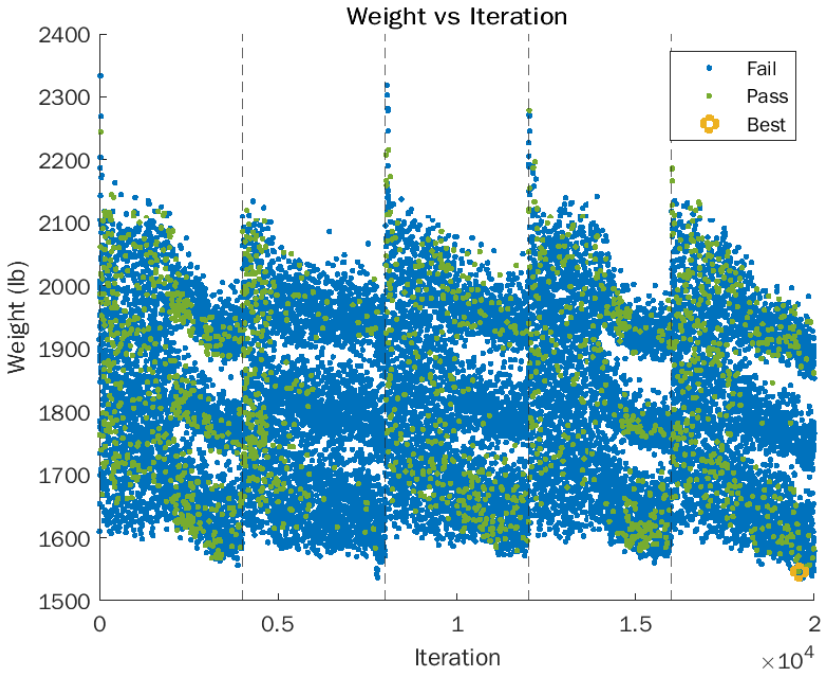

Figure 10. Overview of all 20,000 iterations, demarcated by aircraft that meet requirements (“Pass”) and those that did not (“Fail”). The best aircraft found in the optimization is marked.

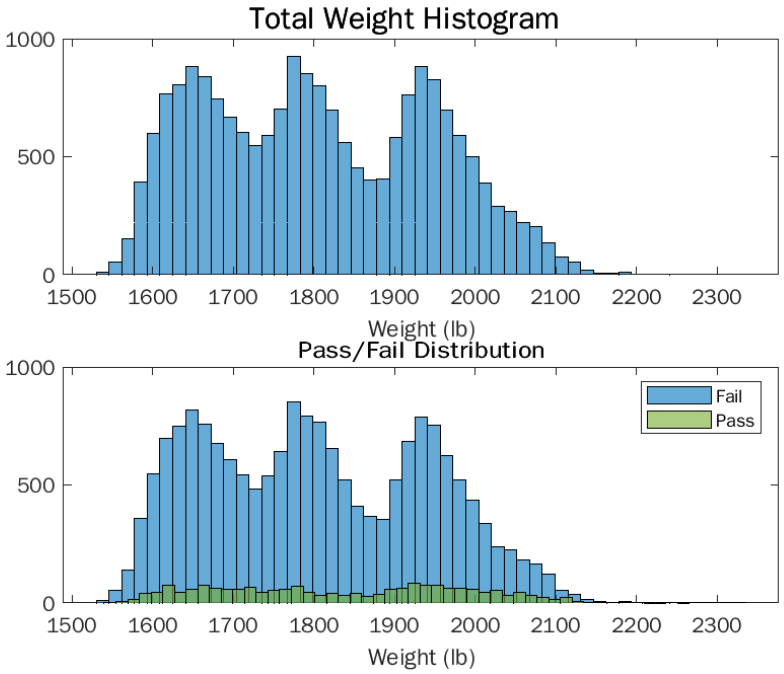

Figure 11. Histogram of all generated aircraft binned by weight. The lower plot breaks down the distribution by Pass and Fail.

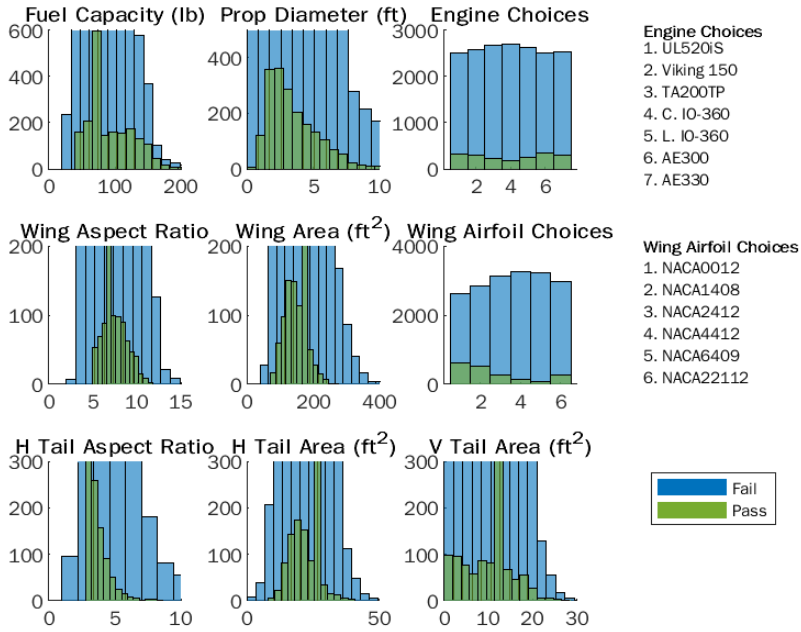

Figure 12. Histograms of aircraft iterations vs aircraft parameters categorized by row: engine and fuel, wing, and tail.

By the histograms, it is seen that all engine choices and wing airfoil choices are capable of yielding aircraft that can pass the requirements and be stable. The pass distribution among the engines indicate that the pass rate among engines are roughly equal, while the pass rate among the airfoils tend to favor airfoils with low camber. For the airfoils, this is likely due to the increase in form (parasitic) drag produced by higher camber airfoils, as seen in with the NACA6409 having the lowest pass rate among all airfoils. High drag would lead to requiring more power and fuel, and thus more weight.

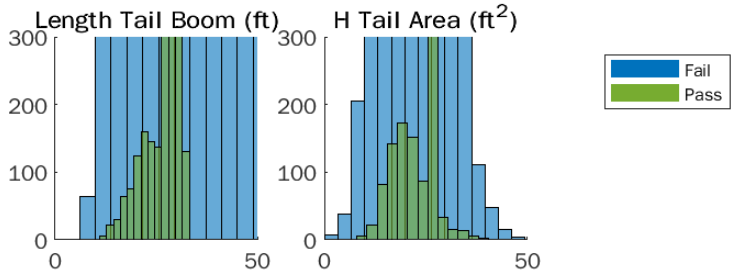

Figure 13. Histograms of aircraft iterations vs aircraft parameters comparing tail boom length and horizontal tail area.

One concern with randomized optimization particularly with randomization on the previous best aircraft is the potential for aircraft geometries to reach extremes, such as the common example of a very long tail boom with a very small tail area to achieve the same moment arm. To prevent this, the randomization of tail boom length is hard-limited and all tail lengths generated longer than the limit is an automatic fail, as seen in Figure 13. Thus, the optimized aircraft keeps a generally reasonable size and geometry.

11. Autonomous Flight and GN&C Strategy

The mission requires the UAV to be based out of LAX and fly to intercept any suspect flying with a jetpack in the vicinity of the LAX airspace. Due to the nature of the heavy traffic and airspace congestion, the UAV must be able to operate within the procedures that airliners would typically operate out of to minimize disruption to commercial traffic. Therefore, the autonomous flight strategy of the UAV can be broken down in the following Table 10, which allows the UAV to be programmed as a state machine.

State	Procedure	GNC Strategy
1. Departure	- Taxi and takeoff (Runway 24L, 25R) - Radar vector departure as instructed by ATC	Waypoint guidance
2. Hunt	- Navigate to suspect's position and maneuver to follow from behind	Dynamic waypoint behind suspect's location
3. Intercept	- Deploy capture net and intercept - Precision targeting with cameras	Dynamic waypoint on suspect's location
4. Return	- Navigate the approach back into LAX following STAR approach as instructed by ATC	Waypoint guidance
5. Arrival	- Final approach and land (Runway 24R, 25L)	Dynamic altitude target to set glideslope

Table 10. Schematic of the UAV autonomy and GNC operating procedure.

For the departure and arrival patterns, the UAV already has all possible ILS procedures pre-programmed in the autopilot memory to allow for instant navigation. In the Simulink simulation, only one departure course (OSHNN ONE) and one STAR arrival course (BASET FIVE) have been programmed in for proof of concept. The procedure charts are shown below in Figure 14 for reference.

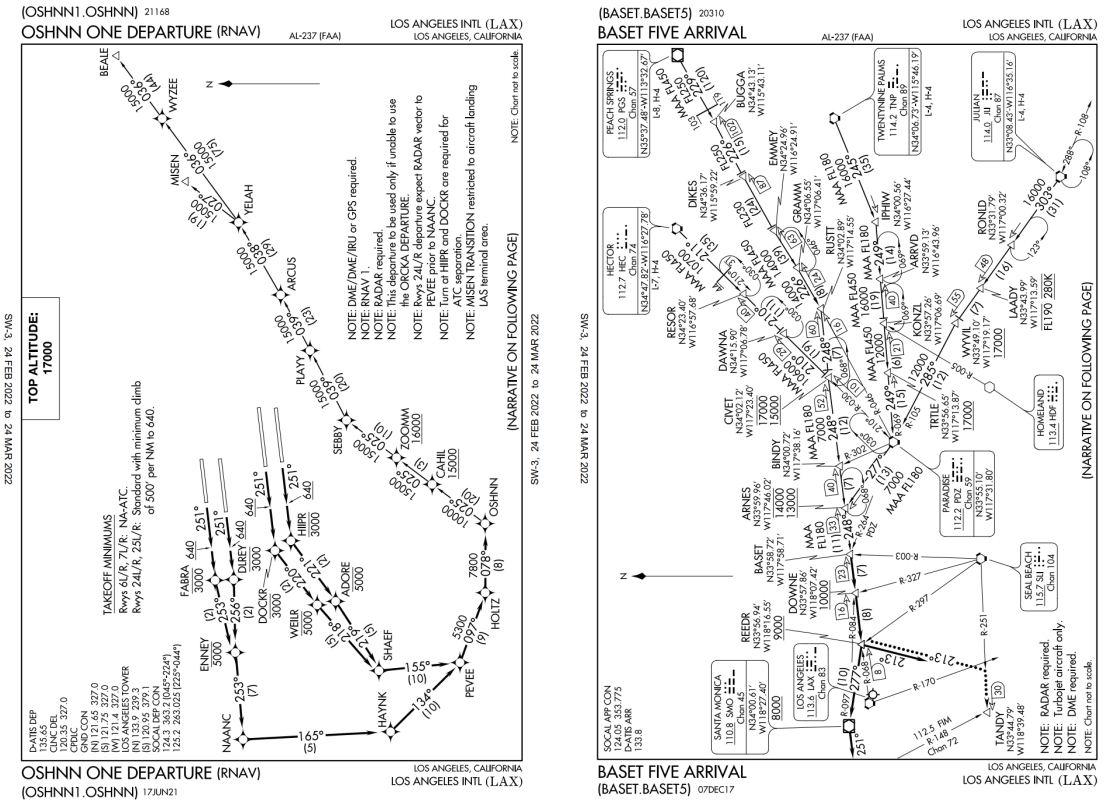

Figure 14. Procedure Charts for the OSHNN ONE Departure (RNAV) and BASET FIVE STAR Arrival, respectively.

One the UAV completes the departure course or is sufficiently in range of the suspect, the UAV departs from the standard course to “hunt” for the suspect. As the UAV flies closer, and with more pilots in the vicinity reporting the suspect on a jetpack’s location, the precise location becomes certain, and the UAV navigates to position itself to fly behind the jetpack, so as to prevent the jetpack from evading.

The intercepting maneuver simply moves the dynamic waypoint from behind the suspect to directly on the suspect. In the Simulink simulation, this is achieved through geospatial coordinates (i.e. position coordinates in the world frame), which are sufficiently accurate as error and noise are not modeled. Realistically, with cameras tracking the suspect, GNC strategies would involve proportional navigation and calculating the collision triangle geometry to ensure that the UAV will intercept the suspect.

However, this control scheme was ultimately not used as the suspect is modeled to move too erratically for the autopilot controller of the UAV to respond fast enough, as the autopilot controller used in the Simulink model is composed of three separate PID controllers for bank angle, airspeed, and altitude. Due to the conflicting controls in airspeed and altitude, which rely on elevator trim and thrust, respectively, the coupled dynamics result in oscillation and transient dynamics that result in imprecise control when the target waypoint is not constant.

With the current control scheme of aligning the UAV behind the suspect, the controller requires less control effort to maneuver the UAV to intercept the suspect. Should the intercept fail, the aircraft will circle back to align itself behind the suspect and attempt again until a successful capture.

The new Simulink waypoint guide block modified from the provided Pioneer UAV Simulink simulation is shown below in Figure 15. Note that the suspect is modeled with random velocities in all three axial directions, with lower frequency speed changes modeled linearly combined with faster varying velocity modeled with Gaussian noise.

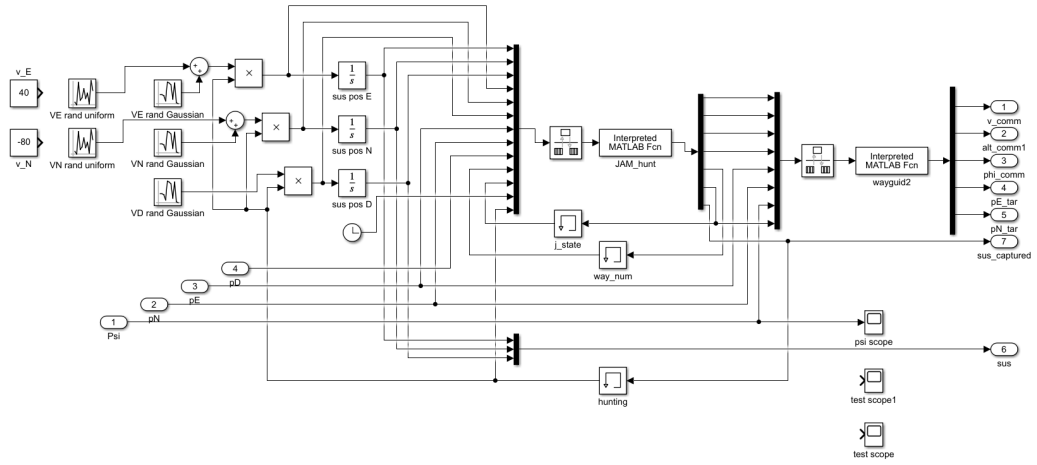

Figure 15. Simulink model of waypoint guide.

12. Conclusion

This aircraft was inspired by the unique news article about the unidentified jetpack flier. The team wanted to design an unique UAV with an unconventional goal of capturing a jetpack suspect. In order to this, several unique requirements had to be defined and the aircraft had to be analyzed for different drag conditions, presenting additional challenges. With some simplifications, the team was able to create a preliminary design, optimizing for weight while fulfilling the requirements defined for successful completion of the mission.

Since this was a preliminary design, the aircraft can be improved upon in future design implementations. The airframe would benefit from a more detailed design, including all the necessary sensors and additional structures to safely apprehend the jetpack person. The flight conditions during the capture of the jetpack person was also not specifically analyzed, and the flight performance of the aircraft while the jetpack capture mechanism is deployed should be carefully analyzed. Overall, the team was excited about the goals of the aircraft and enjoyed learning about the specifics of aircraft design.

Acknowledgements

We would like to thank Professor Damian Toohey and Maharshi Pathak for advising and providing feedback on our design.